Cerebral Cortex February 2014;24:521–531
doi:10.1093/cercor/bhs334
Advance Access publication October 31, 2012

Pansynaptic Enlargement at Adult Cortical Connections Strengthened by Experience

Claire E.J. Cheetham[1,4], Samuel J. Barnes[1], Giorgia Albieri[1], Graham W. Knott[2] and Gerald T. Finnerty[1,3]

[1]MRC Centre for Neurodegeneration Research, King's College London, London, UK [2]Bio-EM Facility, Centre of Interdisciplinary Electron Microscopy, EPFL, Lausanne, Switzerland [3]Department of Clinical Neuroscience (Box 44), Institute of Psychiatry, King's College London, London SE5 8AF, UK [4]Current address: National Institute for Neurological Disorders and Stroke, Bethesda, MD 20892-3703, USA

Address correspondence to Gerald T. Finnerty. Email: gerald.finnerty@kcl.ac.uk

Behavioral experience alters the strength of neuronal connections in adult neocortex. These changes in synaptic strength are thought to be central to experience-dependent plasticity, learning, and memory. However, it is not known how changes in synaptic transmission between neurons become persistent, thereby enabling the storage of previous experience. A long-standing hypothesis is that altered synaptic strength is maintained by structural modifications to synapses. However, the extent of synaptic modifications and the changes in neurotransmission that the modifications support remain unclear. To address these questions, we recorded from pairs of synaptically connected layer 2/3 pyramidal neurons in the barrel cortex and imaged their contacts with high-resolution confocal microscopy after altering sensory experience by whisker trimming. Excitatory connections strengthened by experience exhibited larger axonal varicosities, dendritic spines, and interposed contact zones. Electron microscopy showed that contact zone size was strongly correlated with postsynaptic density area. Therefore, our findings indicate that whole synapses are larger at strengthened connections. Synaptic transmission was both stronger and more reliable following experience-dependent synapse enlargement. Hence, sensory experience modified both presynaptic and postsynaptic function. Our findings suggest that the enlargement of synaptic contacts is an integral part of long-lasting strengthening of cortical connections and, hence, of information storage in the neocortex.

Keywords: barrel cortex, confocal microscopy, electrophysiology, experience-dependent plasticity, structural plasticity

Introduction

The neural basis for information storage in the brain remains a pivotal question in neuroscience. The underlying cellular mechanisms are central to experience-dependent plasticity (Fox and Wong 2005), learning, and memory (Martin et al. 2000). A commonly held hypothesis is that information storage in the nervous system involves a combination of functional and structural modifications to the connections between neurons (Tanzi 1893; Ramón y Cajal 1894; Hebb 1949; Geinisman 2000; Martin et al. 2000; Yuste and Bonhoeffer 2001; Becker et al. 2008; Barnes and Finnerty 2010). The structural modifications may provide a mechanism to maintain long-term alterations in connection strength (Tanzi 1893; Hebb 1949; Geinisman 2000). However, the nature and extent of the structural remodeling involved in information storage remain unclear. One proposal is that the size of existing synapses varies with long-lasting adjustments in function (Tanzi 1893; Hebb 1949). Alternatively, it has been suggested that the number of synapses forming individual connections alters (Ramón y Cajal 1894; Greenough and Bailey 1988). These hypotheses posit that both the strength and structure of connections between pairs of neurons are modified by behavioral experience. This has been extremely hard to demonstrate in mammalian brains (Geinisman 2000; Barnes and Finnerty 2010).

It is widely thought that structure and function are closely related (Lisman and Harris 1993; Pierce and Lewin 1994). In principle, then, it should be possible to predict how behavioral experience alters signaling between neurons from the associated structural modifications to the neuronal connection. Currently, however, it is not known which aspects of the altered synaptic transmission induced by behavioral experience are reinforced by structural remodeling of synapses. Addressing this issue requires a combination of functional recording and morphological reconstruction of the same neuronal connection.

Rodent primary somatosensory cortex (SI) contains an orderly map of the large facial whiskers, with a precise topographic correspondence between the arrangement of the whiskers on the snout and cell clusters in layer 4 of contralateral SI, termed barrels (Woolsey and Van der Loos 1970). This enables the effects of either experience-dependent plasticity or perceptual learning (Guic-Robles et al. 1989; Harris et al. 1999) on the structure–function relationship at synapses to be studied in SI after altering whisker sensory input. Trimming a subset of the whiskers of mature rats for weeks results in strengthening of local excitatory connections between layer 2/3 (L2/3) pyramidal neurons in whisker barrel cortex with retained sensory input (spared cortex; Cheetham et al. 2007). Experience-dependent strengthening occurs without an alteration in the number of putative synapses forming each connection, suggesting that individual synapses are potentiated (Cheetham et al. 2007). Here, we report that the synapses at strengthened connections in spared cortex are larger. We refer to this enlargement as pansynaptic because it encompasses the presynaptic axonal varicosity, the postsynaptic dendritic spine, and the interposed synaptic contact zone. Notably, postsynaptic response amplitude and the reliability of synaptic transmission are also both increased at strengthened connections. Hence, our findings indicate that larger synaptic contacts support enhanced presynaptic and postsynaptic function in the mature cortex.

Materials and Methods

Our experiments were designed to investigate how both function and structure were modified in the same neurons following altered sensory experience (Supplementary Fig. S1). All procedures were performed in accordance with the UK Animals (Scientific Procedures) Act

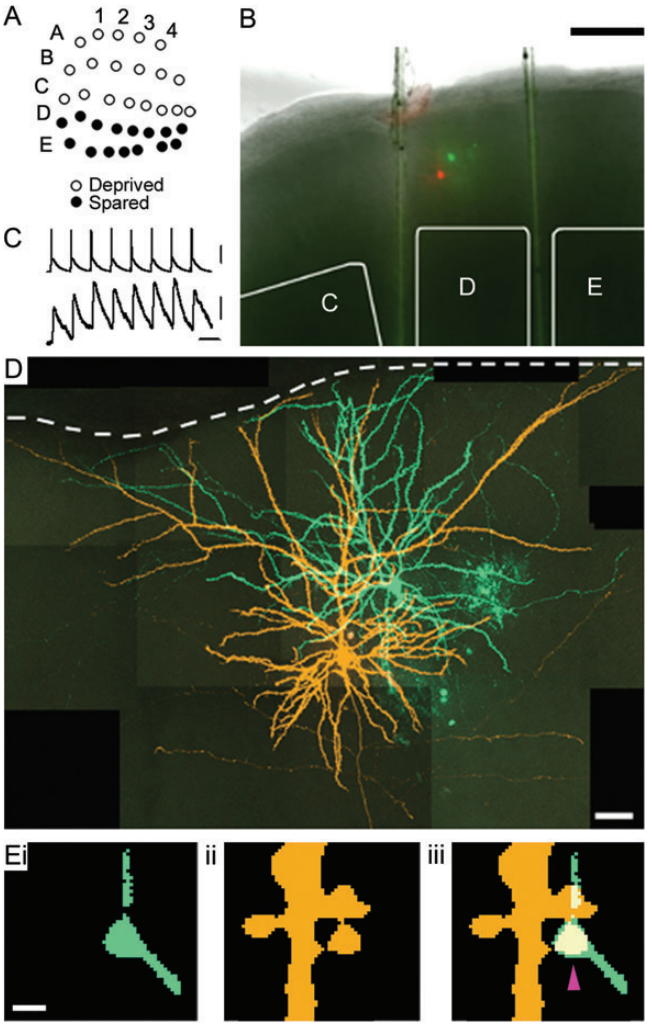

Figure 1. Imaging putative synapses between L2/3 pyramidal neurons. (*A*) Whisker trimming paradigm. An A–C row trim protocol is shown. (*B*) Brain slice showing neurons filled with AF488 (green; presynaptic) and AF568 (red; postsynaptic) in the D (spared) barrel column. Scale bar: 250 μm. (*C*) Train of presynaptic action potentials and postsynaptic excitatory postsynaptic potentials (EPSPs) (average of 50 trials) recorded from the neurons shown in *B*. Scale bars: 40 mV, 0.2 mV; 50 ms. (*D*) A montage of maximum intensity projections of confocal *z*-stacks through the filled neurons shown in *B*. Dashed line indicates the pia. Scale bar: 20 μm. (*E*) Single optical sections showing a presynaptic axonal varicosity (i; green), a postsynaptic dendritic spine (ii; orange), and the interposed contact zone (iii; magenta arrowhead). Scale bar: 1 μm.

of 1986 and the European Communities Council Directive of 24 November 1986 (86/609/EEC). All necessary measures were taken to minimize pain and discomfort.

Whisker Trimming

Altered sensory experience was induced by bilateral trimming of either the upper 3 rows (A, B, and C rows and α, β, and γ outliers termed A–C row trim) or the lower 2 rows (D and E rows, γ and δ outliers termed D–E row trim) of rats' whiskers daily from P19 for 13–41 days ($n = 12$ rats). Sham-trimmed littermates ($n = 13$ rats) were used as controls. On the day of the experiment, all whiskers were acutely trimmed by an assistant to blind the experimenter to the rat's sensory experience during electrophysiological recording, imaging, and analysis.

Brain Slice Preparation and Recording

Brain slices were cut across the whisker barrel rows (65° to the midline; Cheetham et al. 2007). We made whole-cell voltage recordings from pairs of synaptically connected L2/3 pyramidal neurons in spared and control cortex at 36–37°C. Pairs of neurons in spared cortex were recorded from either the D barrel column in slices from A–C row trimmed rats ($n = 9$; Fig. 1*A*), or the C barrel column in slices from D–E row trimmed rats ($n = 3$). Pairs of neurons in control cortex were recorded in either the C or the D barrel column of slices from sham-trimmed rats. Presynaptic and postsynaptic neurons were filled with different fluorescent dyes (AF488 or AF568, Invitrogen) during recording, enabling the identification of the putative synapses connecting them. Although it is possible that some synapses between connected pairs of neurons were lost as a result of slicing, these synapses would not have contributed to the electrophysiological recordings and, hence, their loss would not affect our analyses. Our brain slice preparation protocol results in spine densities on L2/3 pyramidal neurons (Cheetham et al. 2008) that are similar to those measured after perfusion–fixation of the neocortex (Peters and Kaiserman-Abramof 1970; Wise et al. 1979; Larkman 1991; Wallace and Bear 2004) and, hence, indicate that our brain slice preparation does not cause a proliferation of spines on L2/3 pyramidal neurons, as reported for hippocampal pyramidal neurons (Kirov et al. 1999). For a subset of connections, recordings were made sequentially in normal artificial cerebrospinal fluid (ACSF, which contains 2 mM $CaCl_2$) and in ACSF containing 5 mM $CaCl_2$.

Electrophysiological Analysis

Single-axon connections between pairs of neurons termed unitary excitatory postsynaptic potentials (uEPSPs) were analyzed as described previously (Cheetham et al. 2007). We defined an evoked uEPSP as having 2 properties with respect to the average of 50 traces: 1) The latency of the response to an action potential in the presynaptic neuron fell within ±0.6 ms of the latency of the mean uEPSP and 2) the peak of the evoked response was within ±1.0 ms of the peak of the mean uEPSP. Spontaneous EPSPs were defined as EPSPs that did not fulfil the criteria for an evoked response. Failures were defined as traces that had no evoked uEPSP. Failures were scored independently by 2 people and any discrepancies were rechecked. Failure traces for each connection were then averaged to ensure that small responses had not been missed. The probability of failure was calculated from responses to the first action potential in the stimulus train. The coefficient of variation was calculated as the standard deviation of single uEPSP responses for a connection divided by the mean uEPSP amplitude for that connection. The maximum evoked uEPSP amplitude was defined as the mean of the 3 largest responses from typically 50–150 trains of 8 action potentials (minimum, 20 trains). The maximum evoked uEPSP amplitude per synapse was calculated by dividing the maximum evoked uEPSP amplitude by the anatomically determined number of putative synapses forming the connection to estimate the contribution of a theoretical "average" synapse to the uEPSP amplitude.

Confocal Imaging and Image Processing

Presynaptic and postsynaptic neurons were filled with different fluorescent dyes during recording. Following electrophysiological recording, slices were fixed in 4% paraformaldehyde at room temperature for 30 min, washed in phosphate-buffered saline (PBS), and mounted using Gel/Mount (Invitrogen). We used a Zeiss 510 META confocal microscope with a C-Apochromat ×63, 1.2 numerical aperture water-immersion objective with coverslip correction. Pinhole diameters were set to give an identical optical slice thickness for both channels (0.43 μm; AF488, 1 Airy unit; AF568, 0.84 Airy units). Medium resolution *z*-stacks (≤120 μm; voxel, 0.14 × 0.14 × 0.43 μm; Supplementary Movie S1) encompassing the entire postsynaptic dendritic arbor were acquired and examined for the presence of possible synapses. All regions where presynaptic axon passed close to a postsynaptic dendrite were reimaged at high resolution (voxel, 0.07 × 0.07 × 0.20 μm; intensity, 8 bit) with 8× mean averaging. For clarity of presentation,

presynaptic neurons have been pseudocolored green, and postsynaptic neurons have been pseudocolored orange.

We deconvolved our images using a blind adaptive point spread function (PSF) algorithm (AutoDeblur, Media Cybernetics, Bethesda, MD, United States of America; Landmann and Marbet 2004; Supplementary Fig. S2). Image-processing parameters were determined from the measurements of 0.10–1.00 μm diameter fluorescent beads (TetraSpeck, Invitrogen) made in the higher resolution *xy* plane, which showed that 10 iterations of deconvolution and a minimum fluorescence intensity threshold of 25% were optimal, that is, the full-width quarter-maximum diameter provided the most accurate measurement of the imaged structure (Supplementary Fig. S3). Therefore, images of possible synapses underwent 10 iterations of deconvolution and were thresholded at 25% of the maximum fluorescence intensity of the imaged structure. This enabled us to measure the volumes of the axonal varicosities and dendritic spines that formed the putative synapses and to quantify the number of colocalized fluorescence voxels comprising the interposed contact zones. Measurements from the deconvolved and thresholded images were made using Measurement Pro running under Imaris x64 (Bitplane, Zurich, Switzerland), ImageJ v1.36–1.43 (http://rsb.info.nih.gov/ij), and Fiji (http://fiji.sc/wiki/index.php/Fiji).

Image Resolution

We measured the PSF of our imaging system using 0.10 μm diameter beads (TetraSpeck, Invitrogen), which are loaded with fluorescent dyes with similar absorption and emission peaks to the AF488 and AF568 used to fill neurons (Supplementary Fig. S3*A*,*B*). The size of the PSF is usually measured by the full-width half-maximum (FWHM) and increases with imaging wavelength. Therefore, the signal from the AF568 dye limits the resolution achievable in our neuronal images. Accordingly, we used the bead emission at >560 nm for PSF measurements. The FWHMs of each PSF were measured in Fiji using the MetroloJ plugin (http://imagejdocu.tudor.lu/doku.php?id=plugin:analysis:metroloj:start). The FWHM of 0.10 μm diameter beads ($n = 15$) before deconvolution was 0.24 [0.20–0.25] μm in the *xy* plane and 0.76 [0.66–0.79] μm in the *z*-axis. This decreased to 0.17 [0.16–0.19] μm in the *xy* plane and 0.48 [0.44–0.53] μm in the *z*-axis after 10 iterations of deconvolution.

The deconvolution software (AutoDeblur) returned not only the image of the deconvolved structures, but also the PSF used for deconvolution. We compared the measured PSF of 0.10 μm beads in the *xy* plane with the PSF in the *xy* plane estimated by the deconvolution software to determine how accurately the software estimated the measured PSF and found that the 2 values were in good agreement (AutoDeblur PSF, 0.17 μm). Therefore, we used the AutoDeblur PSF in the *xy* plane to monitor the effect of imaging putative synapses in tissue. We found that the AutoDeblur PSF enlarged to a maximum of 0.19 μm in the *xy* plane when imaging filled neurons in brain slices. These data indicate that resolution is slightly reduced when imaging neurons in lightly fixed brain slices, but that the FWHM in the *xy* plane remains below the diameter of the smallest synaptic contact zones that we and others have found with electron microscopy (EM) (Peters and Kaiserman-Abramof 1969; Jones and Calverley 1991).

We assessed how accurately our imaging system could measure objects near the limit of light resolution by imaging fluorescent beads of similar sizes to synapses (Supplementary Fig. S3*C*–*E*). Importantly, differences between the measured volumes of beads of different diameters (0.10, 0.50, and 1.00 μm) were significant ($P = 0.002$, 1-way analysis of variance [ANOVA] on ranks; $P < 0.05$ for all pairwise comparisons with the Student–Newman–Keuls method, $n = 5$ beads per group). The standard deviation of the diameter of 0.50 μm beads measured in the *xy* plane with confocal microscopy was small and was comparable with the manufacturer's data from EM measurements (manufacturer's standard deviation = 0.02 μm; our data = 0.03 μm). Hence, our imaging system has the sensitivity to detect differences at the submicrometer level.

High-resolution confocal imaging overestimates the volume of structures near the resolution of light because the image is stretched in the *z*-axis. Therefore, as an additional check of the robustness of our findings, we used fluorescent beads with diameters similar to those of contact zones measured with EM (Jones and Calverley 1991), to correct for the volume overestimation attributable to fluorescence imaging. We fitted a power law function to the relationship between real and measured bead volumes (measured volume = 3.74(real volume)$^{0.92}$, $R^2 = 0.997$; Supplementary Fig. S6*A*). We then used this function to calculate the corrected contact zone sizes for putative synapses in control and spared cortex (Supplementary Fig. S6*B*).

Classification and Measurement of Dendritic Spines and Axonal Varicosities

Putative synapse-forming spines were classified as mushroom, stubby, or thin, using criteria similar to those described previously (Peters and Kaiserman-Abramof 1970; Harris et al. 1992; Knott et al. 2006). Thin spines had lengths much greater than their diameters, and similar head and neck diameters. Mushroom spines had a much greater head than neck diameter, and stubby spines had a similar length and diameter. Dendritic protrusions characterized as filopodia (thin neck >3 μm in length and no head) were rare and did not form identified putative synapses. The boundaries of spines relative to the dendritic shaft were defined by extending a line, parallel to the direction of travel of the dendrite, which linked the points where the spine emerged from the dendrite, for each optical section. Spines were excluded from analysis if they merged with a neighboring spine or protruded from the dendrite primarily in the *z*-axis such that the limits of the spine relative to the shaft could not be determined. Axonal varicosities were defined as swellings of the axonal shaft with a varicosity diameter ≥1.25 times the diameter of the adjacent axonal shaft and fluorescence signal in the varicosity ≥1.30 greater than that of the adjacent axonal shaft (Cheetham et al. 2008). The boundaries between a varicosity and the adjacent axonal shaft were defined as a points where the transverse diameter of the varicosity increased above the diameter of the adjacent axonal shaft in each optical section. The volume of each spine or varicosity was calculated by measuring the area of the spine/varicosity fluorescence in contiguous optical sections, multiplied by the *z*-step (0.20 μm), and summed to give a fluorescence volume.

Identifying Putative Synapses with Light

We have described previously criteria for identifying putative synapses between neurons, which are filled with different fluorophores and are known to be synaptically connected from electrophysiological recording (Cheetham et al. 2007). After high-resolution confocal imaging of the neurons and image deconvolution, our putative synapse identification criteria require that: 1) A presynaptic axonal varicosity (Cheetham et al. 2008) and a postsynaptic dendritic spine or shaft form an overlap that has a minimum diameter of 0.40 μm in the higher resolution *xy* plane (Supplementary Results) and 2) the overlap extends through at least 4 contiguous 0.20 μm optical sections in the lower resolution *z*-axis.

We have previously tested our optical criteria for the identification of putative synapses by reconstructing the overlaps between axons and dendrites of L2/3 pyramidal neurons that were not synaptically connected and estimate that our criteria have a false-positive rate of 5% (Cheetham et al. 2007). For this analysis, we reconstructed either the unconnected direction from pairs of unidirectionally connected L2/3 pyramidal neurons ($n = 8$) or pairs of unconnected L2/3 pyramidal neurons ($n = 2$). A pair or direction was termed "unconnected" when both cells were recorded in whole-cell mode, and action potentials in 1 neuron failed to evoke EPSPs in the other neuron. A minimum of 20 stimulus trains, each of which evoked 8 action potentials at 20 Hz in the "presynaptic" neuron, were recorded and examined individually and as averages to ensure that weak or facilitating connections were not missed. Unconnected pairs and directions were reconstructed in the same way as described for the connected pairs of neurons: Medium resolution *z*-stacks (≤120 μm; voxel, 0.14 × 0.14 × 0.43 μm; Supplementary Movie S1) encompassing the entire dendritic arbor of both neurons were acquired and examined for the presence of possible synapses. All regions where the axon of one neuron passed close to a dendrite of the other neuron were

reimaged at high resolution (voxel, 0.07 × 0.07 × 0.20 μm; intensity, 8 bit) with 8× mean averaging, and these images were deconvolved. False-positive putative synapses fulfilled the criteria for a putative synapse listed above.

The volume of each contact zone was calculated by measuring the number of colocalized pixels in each contiguous optical section (Supplementary Fig. S2) and summing them to give the contact zone size in voxels. Colocalized voxels contributed to the contact zone only if they fell within the boundaries of the varicosity and spine (for putative synapses on dendritic spines) forming the putative synapse. The mean contact zone size did not differ between pairs in spared cortex of A–C trimmed and D–E trimmed rats ($P = 0.37$, Mann–Whitney rank sum test). Therefore, data from A–C and D–E trimmed rats were pooled.

We found that each contact zone comprised at least 40 voxels (voxel, 0.07 × 0.07 × 0.20 μm). Connections between pairs of pyramidal neurons consist of 1–10 synapses distributed over the dendritic tree (Markram et al. 1997; Silver et al. 2003; Cheetham et al. 2007). Furthermore, we recorded only 1 synaptically connected pair of neurons in each brain slice and filled presynaptic and postsynaptic neurons with different fluorescent dyes. Hence, only 1 fluorescently labeled synapse is likely to be present in each imaging voxel. These data indicate that our imaging protocol is capable of visualizing the smallest neocortical synapses.

Contact Zone Size and Probability of Failure

The relationship between contact zone size and the probability of failure at a connection was well fitted by a theoretically derived power relationship:

$$\text{Probability of failure} = (1 - k(\text{mean contact zone size}))^n$$

where n is the anatomically determined number of putative synapses forming the connection, mean contact zone size is the mean contact zone size for the putative synapses forming the connection, and k is a constant. The probability of failure at a connection is approximated by $(1–p)^n$, where p is the average probability of release of the synapses forming the connection and n is the number of synapses forming the connection. The equation assumes that the size of the contact zone is proportional to the probability of release of that synapse. This assumption is based on the findings that the contact zone scales with the presynaptic active zone, whose area correlates with the probability of release (Peters and Kaiserman-Abramof 1969; Dyson and Jones 1980; Jones and Calverley 1991; Pierce and Lewin 1994; Harris and Sultan 1995; Dobrunz and Stevens 1997; Schikorski and Stevens 1997; Murthy et al. 2001; Schikorski and Stevens 2001). Furthermore, the probability of release at many synapses is linearly related to the volume of the presynaptic varicosity (Pierce and Lewin 1994), and we show that varicosity volume is linearly related to contact zone size (Fig. 3*C*). Fitting the equation to our data returned $k = 0.0017$ ($P < 0.001$, $R^2 = 0.48$). For display purposes, the curve shown in Figure 5*D* was calculated using $n = 3.65$, the mean putative synapse number for all connections.

Electron Microscopy

A P60 rat was transcardially perfused with 500 mL fresh fixative (4% paraformaldehyde and 0.2% EM-grade glutaraldehyde in 0.1 M phosphate buffer [PB], pH 7.4). Brains were embedded in 5% agarose in PB (0.1 M, pH 7.4), and 60 μm slices cut across the whisker barrel rows (65° to the midline) in PBS (0.1 M PB, 0.9% NaCl, pH 7.4) using a VT1000S vibratome (Leica Microsystems). Slices were then washed in sodium cacodylate buffer (0.1 M, pH 7.4), stained in osmium tetroxide with potassium ferrocyanide followed by osmium tetroxide, and then uranyl acetate. Stained sections were embedded in Durcupan resin and cured for 24 h at 65°C. The region of interest was cut from the hardened section and serially sectioned at 50 nm thickness. The sections were collected on single-slot grids, stained with lead citrate, and then imaged in a CM10 transmission electron microscope (operating at 80 kV tension) with a digital camera (Morada, Olympus). Image alignment and morphological analysis, for example, apposition surface, synaptic surface, and synapse density, were carried out in Fiji running the TrakEM2 plugin. A grid method was used to count the number of asymmetric (presumed excitatory) synapses and the total number of instances where boutons and spines were apposed, but no synapse was present. The area of either a bouton–spine contact zone or postsynaptic density (PSD) was measured in each EM image in which it was present, and summed to give the total surface area in 3 dimensions.

Statistics

Normally distributed data were described by their mean ± standard error of the mean and were analyzed using *t*-tests or 2-way ANOVAs and linear regression. Data that failed normality and/or equal variance tests were expressed as median [interquartile range]. Where possible, these data either underwent a natural log transform to normalize their distributions and/or equalize their variances prior to performing *t*-tests, ANOVA, or linear regression. Alternatively, they were analyzed with a Mann–Whitney rank sum test, 1-way ANOVA on ranks, or Spearman's rank correlation coefficient. Outliers (1 control and 1 spared putative synapse) were defined as data points outside the range encompassed by the mean ± three standard deviations and were excluded from the structural analysis. Percentage differences in sizes are given as the percentage difference between the mean values for the 2 groups if both were normally distributed with equal variances, or otherwise as the percentage difference between median values. Distributions were compared using Kolmogorov–Smirnov or Andersen–Darling tests (Cheetham et al. 2007; Matlab, Mathworks). All statistical tests were 2-tailed with alpha set at 0.05.

Data were from 13 connected pairs comprising a total of 40 putative synapses in control cortex and from 12 connected pairs comprising a total of 44 putative synapses in spared cortex. Values for n, which are quoted in the Results, differed between data sets because: 1) Not all putative synapses were formed on dendritic spines (36 putative synapses in control cortex and 31 putative synapses in spared cortex were formed on dendritic spines) and 2) not all spines could be measured because the spine merged with a neighboring spine or the spine and dendritic shaft were aligned in the *z*-axis (27 of 36 putative synapse-forming spines in control cortex and 25 of 31 putative synapse-forming spines in spared cortex were measured). Two reconstructed connections in spared cortex were excluded from the probability of release, coefficient of variation, and maximum evoked EPSP amplitude analyses because either the presynaptic or the postsynaptic resting membrane potential was not stable (depolarized above −65 mV) during the recording period.

The relationships between the area of the postsynaptic density and the area of the contact zone from our EM measurements; spine volume and varicosity volume from our confocal images; and age and the size of the varicosity, spine, or contact zone were modeled under the generalized linear model framework using the "stat" package in R (R Project for Statistical Computing; http://www.r-project.org), as described previously (Cheetham et al. 2008). The models were, respectively,

$$E(\text{postsynaptic density area}) = \alpha + \beta_1(\text{contact zone area})$$

with the Gamma error family where E(postsynaptic density area) is the expected area of the postsynaptic density, α and β_1 are coefficients of the model;

$$E(\text{varicosity volume}) = \alpha + \beta_1(\text{spine volume}) + \beta_2(\text{SP})$$

with the Gaussian error family where E(varicosity volume) is the expected volume of the varicosity, α, β_1, and β_2 are coefficients of the model, and SP is a dummy explanatory variable denoting L2/3 pyramidal neurons in spared cortex (spared = 1, control = 0); and

$$E(\text{size}) = \alpha + \beta_1(\text{age}) + \beta_2(\text{SP} \times \text{age})$$

with the Gaussian error family where E(size) is the expected volume of the varicosity, spine, or contact zone, age is the age of the rat on the day of recording, α, β_1, and β_2 are coefficients of the model, and SP is a dummy explanatory variable denoting L2/3 pyramidal neurons in

spared cortex (spared = 1, control = 0). (SP × age) denotes the interaction between spared cortex and age. The strengths of the linear relationships were reported using the explained deviance as a percentage of the null deviance. This is the equivalent in linear regression of the coefficient of determination, R^2, which is a measure of the variance in the data explained by the linear regression model.

Varicosity–contact zone and spine–contact zone relationships from our fluorescence data were modeled under the generalized estimating equations framework using the "stat" and "gee" packages implemented in R (Cheetham et al. 2008). The models were:

$$E(\text{contact zone voxels}) = \alpha + \beta_1(\text{varicosity volume}) + \beta_2(\text{SP}) + \beta_3(\text{SHAFT})$$

$$E(\text{contact zone voxels}) = \alpha + \beta_1(\text{spine volume}) + \beta_2(\text{SP} \times \text{spine volume})$$

with the Gamma error family and unstructured working correlation matrices. E(contact zone voxels) is the expected size of the contact zone in fluorescence images, α, β_1, β_2, and β_3 are coefficients of the model, varicosity and spine volume are the volumes of the varicosities and spines, respectively, and (SP × spine volume) denotes the interaction between spared cortex and spine volume. SP is a dummy explanatory variable denoting L2/3 pyramidal neurons in spared cortex (spared = 1, control = 0). SHAFT is a dummy explanatory variable representing putative synapses formed on the dendritic shaft (putative shaft synapse = 1, putative spine synapse = 0). Model selection was performed by minimizing the quasi-likelihood criterion (Pan 2001). Two-tailed P-values were calculated using the robust (sandwich) estimate of variance.

Results

Altering whisker experience leads to the strengthening of local excitatory connections between L2/3 pyramidal neurons in spared cortex (Cheetham et al. 2007). To investigate the role of structural remodeling in this synaptic strengthening, we prepared brain slices and recorded synaptically connected pairs of L2/3 pyramidal neurons in spared cortex of trimmed rats, or control cortex of sham-trimmed rats (Fig. 1*A–C*, Supplementary Fig. S1). Presynaptic and postsynaptic neurons were filled with different fluorescent dyes during recording and visualized using high-resolution laser-scanning confocal microscopy. The images were deconvolved prior to reconstruction in three-dimensions (3D) (Fig. 1*D*, Supplementary Figs S2 and S3; Materials and Methods). This enabled us to identify the putative synapses forming local excitatory connections between L2/3 pyramidal neurons (Fig. 1*E*), using criteria validated previously (Cheetham et al. 2007). All electrophysiological recordings, imaging, and analysis were performed blind to the animal's sensory experience (Cheetham et al. 2007).

We found that putative synapse number per connection was very similar in control cortex (median [interquartile range]: 3 [1–4] putative synapses per connection, $n = 13$ connections) and in spared cortex (3 [2–4] putative synapses per connection, $n = 12$ connections; $P = 0.78$, Mann–Whitney rank sum test), as we have reported previously (Cheetham et al. 2007). There were no differences in the passive membrane properties, location, or dendritic morphology of recorded neurons in control and spared cortex (Supplementary Table S1). Therefore, our data suggest that the experience-dependent strengthening of connections between L2/3 neurons in spared cortex (see below) is attributable to potentiation of the synapses forming those strengthened connections (Cheetham et al. 2007).

Axonal Varicosities Forming Putative Local Excitatory Synapses are Larger in Spared Cortex

Stronger excitatory connections in spared cortex show greater short-term depression of synaptic responses when the presynaptic neuron fires a train of action potentials (Cheetham et al. 2007). This is thought to reflect altered function of the presynaptic terminal (Zucker and Regehr 2002). Therefore, we investigated whether sensory experience modified the structure of axonal varicosities, which form the presynaptic terminals, at putative synapses in spared cortex. We measured the volumes of all axonal varicosities that formed putative synapses between the pairs of L2/3 pyramidal neurons that we had recorded from (Fig. 2*A*). Varicosities forming putative local excitatory synapses between L2/3 pyramidal neurons were 62% larger in spared cortex (0.52 [0.26–0.98] μm^3, $n = 44$) than in control cortex (0.32 [0.21–0.57] μm^3, $n = 40$; $P = 0.019$, t-test, Materials and Methods; Fig. 2*B*, Supplementary Fig. S4*A*, *B*). The distribution of varicosity volumes was also tilted to larger volumes in spared cortex (Fig. 2*B*; $P = 0.020$, Andersen–Darling test). This finding indicated that the increase in size of

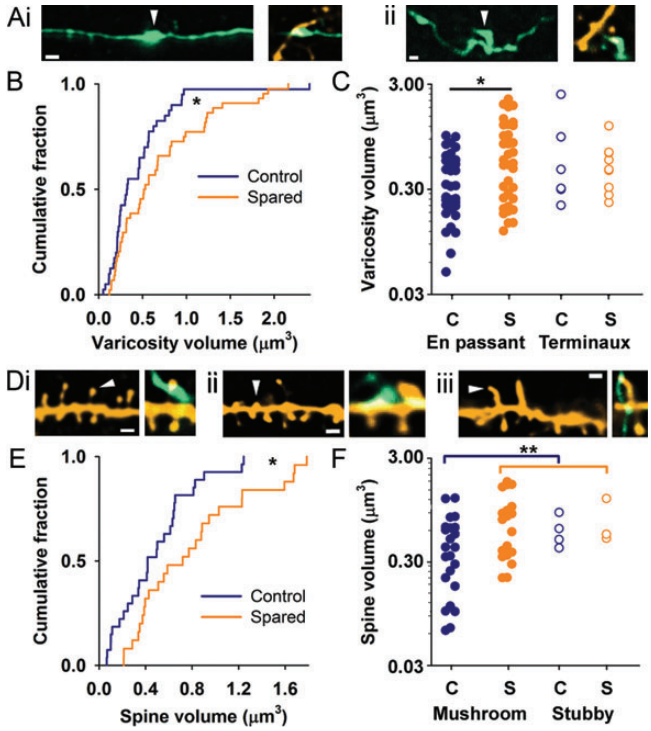

Figure 2. Axonal varicosities and dendritic spines are larger in spared cortex. (*A*) Left panels show maximum intensity projections of segments of axon in spared cortex. Arrowheads indicate en passant (i) and terminaux (ii) varicosities that form putative synapses. Right panels show single optical sections through the putative synapses formed by these varicosities. Scale bars: 1 μm. (*B*) Empirical distribution functions for the volumes of putative synapse-forming varicosities in control ($n = 40$ varicosities from 13 connections) and spared ($n = 44$ varicosities from 12 connections) cortex. *$P = 0.020$, Andersen–Darling test. (*C*) Volumes of en passant and terminaux varicosities forming putative synapses. Note: log scale, *$P = 0.010$, t-test. (*D*) Left panels show single optical sections through segments of dendrite from spared cortex. Arrowheads indicate mushroom (i), stubby (ii), and thin (iii) spines that form putative synapses. Right panels show single optical sections through the putative synapses formed by these spines. Scale bars: 1 μm. (*E*) Empirical distribution functions for the volumes of putative synapse-forming dendritic spines in control ($n = 27$ spines from 13 connections) and spared ($n = 25$ spines from 12 connections) cortex. *$P = 0.038$, Kolmogorov–Smirnov test. (*F*) Volumes of mushroom and stubby spines forming putative synapses. Note: log scale, **$P = 0.007$ for spines in control versus spared cortex, 2-way ANOVA.

varicosities forming strengthened local excitatory connections in L2/3 of spared cortex could not be attributed to the extensive expansion of just a subset of those varicosities.

Axonal varicosities either emerge directly from the axon shaft (en passant) or form at the end of protrusions from the axon shaft (terminaux; Fig. 2*A*). En passant varicosities that formed putative synapses between L2/3 pyramidal neurons were 72% larger in spared cortex (0.55 [0.25–1.22] μm^3, $n = 35$) than in control cortex (0.32 [0.21–0.56] μm^3, $n = 34$; $P = 0.010$, *t*-test; Fig. 2*C*). Terminaux varicosities were 20% larger in spared cortex (0.46 [0.31–0.57] μm^3, $n = 9$) than in control cortex (0.38 [0.30–0.70] μm^3, $n = 6$; $P = 0.80$, *t*-test; Fig. 2*C*), but this result did not attain statistical significance, possibly due to the small data set for terminaux varicosities at identified putative synapses. Varicosity volume in spared cortex increased with the duration of whisker deprivation (Supplementary Fig. S5*A*). Taken together, our findings suggested that experience-dependent strengthening of local excitatory connections was accompanied by the progressive enlargement of the presynaptic axonal varicosities that form those connections.

Dendritic Spines Forming Putative Local Excitatory Synapses are Larger in Spared Cortex

Most cortical excitatory synapses are formed on dendritic spines (Elhanany and White 1990; Knott et al. 2006). Synaptic strengthening induced by long-term potentiation (LTP) has been reported to cause spine enlargement (Fifková and Van Harreveld 1977; Matsuzaki et al. 2004; Park et al. 2004; Kopec et al. 2007; Tanaka et al. 2008). However, there is conflicting evidence as to whether LTP-induced spine expansion is long-lasting at mature synapses (Sorra and Harris 1998; Lang et al. 2004; Bozdagi et al. 2010). Therefore, we explored how spines forming putative local excitatory synapses between L2/3 pyramidal neurons were modified by sensory experience (Fig. 2*D*). Dendritic spines were 72% larger in spared cortex (0.72 [0.38–1.08] μm^3, $n = 25$) than in control cortex (0.42 [0.22–0.65] μm^3, $n = 27$; $P = 0.008$, *t*-test; Fig. 2*E*, Supplementary Fig. S4*C*,*D*). The distribution of dendritic spine volumes was also shifted toward larger values ($P = 0.038$, Kolmogorov–Smirnov test; Fig. 2*E*). This finding indicated that most dendritic spines forming strengthened local excitatory connections in spared cortex were larger, rather than there being expansion of just a subset of those dendritic spines.

It has been proposed that LTP-induced spine enlargement may preferentially affect small spines (Matsuzaki et al. 2004). It remains uncertain whether dendritic spines on neocortical neurons can be subdivided into clearly distinguishable groups or whether they form a continuum of shapes and sizes (Wallace and Bear 2004; Arellano et al. 2007). However, the classification of spines into mushroom, stubby, and thin types (Peters and Kaiserman-Abramof 1970) remains widely recognized. The proportions of different spine types (Fig. 2*D*) forming putative synapses between L2/3 pyramidal neurons were similar in control cortex (80% mushroom, 20% stubby, $n = 36$) and in spared cortex (69% mushroom, 25% stubby, 6% thin, $n = 31$; $P = 0.91$, χ^2 test). Further analysis indicated that the sizes of different spine types were affected similarly by altered whisker experience (Fig. 2*F*; $P = 0.78$ for spine type, $P = 0.007$ for spared vs. control, 2-way ANOVA). Statistical modeling did not suggest a clear temporal profile for spine enlargement (Supplementary Fig. S5*B*). We concluded that the volumes of all spine types were increased during experience-dependent strengthening of local excitatory cortical connections.

Contact Zones are Larger in Spared Cortex

We next investigated whether the size of the contact between a presynaptic varicosity and a postsynaptic dendrite was also altered at strengthened connections in spared cortex. For any putative synapse, the apposition of an axonal varicosity and a dendrite will be visible in a fluorescence image as an overlap of that varicosity and dendrite (Cheetham et al. 2007; Fig. 3*A*). This overlap is a consequence of the closeness (≤30 nm) of axon and dendrite at contacts. EM studies show that the diameter of the apposition between a presynaptic varicosity and a postsynaptic dendrite at excitatory synapses in L2/3 of mature SI is ≥0.25 μm (Peters and Kaiserman-Abramof 1969; Jones and Calverley 1991). This is above the resolution of our fluorescence images (Materials and Methods) and suggests 2 important conclusions: first, our fluorescence images would not miss the smallest contacts between neurons and; second, the fluorescence overlap at contacts can be used as an index of the size of those contacts. Therefore, we measured the size of these overlaps in 3D by counting the number of colocalized voxels.

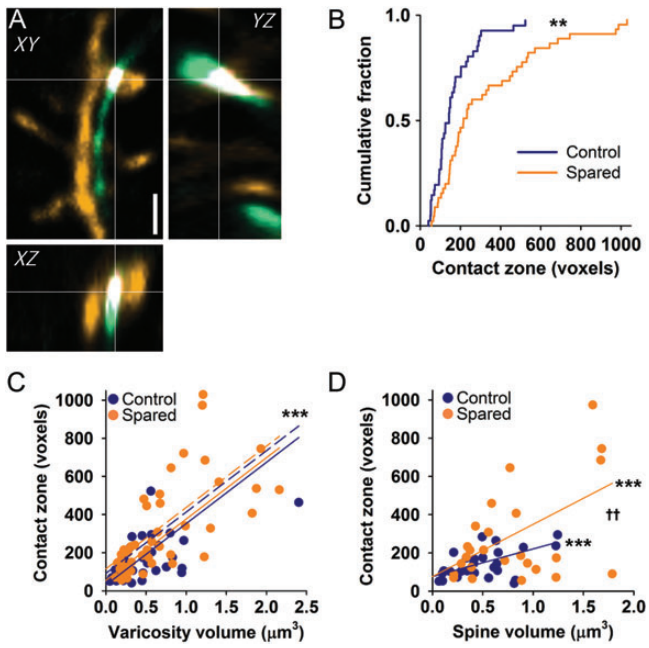

Figure 3. Contact zones are larger in spared cortex. (*A*) Example of a putative local excitatory synapse from control cortex. The contact zone (white) has been projected onto 3 planes (left, *XY*; right, *YZ*; lower, *XZ*). Scale bar: 1 μm. (*B*) Empirical distribution functions for contact zone size in control ($n = 40$ putative synapses from 13 connections) and spared ($n = 44$ putative synapses from 12 connections) cortex. $^{**}P = 0.006$, Kolmogorov–Smirnov test. (*C*) Relationship between contact zone size and varicosity volume for individual putative synapses. Voxels are ~0.001 μm^3. Lines represent generalized estimating equation fits: *E*(contact zone voxels) = 29.8 + 313 (varicosity volume) + 23.8(SP) + 58.5(SHAFT) for putative synapses formed on dendritic spines (solid) and dendritic shafts (dashed). $^{***}P < 0.001$ for slope for all groups. (*D*) Relationship between contact zone size and spine volume for individual putative synapses. Lines represent generalized estimating equation fits: *E*(contact zone voxels) = 74.4 + 140(spine volume) + 125(SP × spine volume); $^{***}P < 0.001$ for the slope for both groups; $^{††}P = 0.002$ for control versus spared.

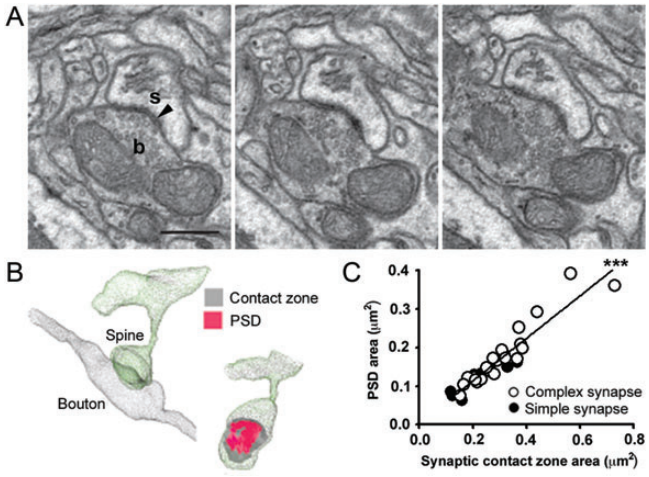

Figure 4. Contact zone size scales with synapse size in spared cortex. (*A*) Three consecutive EM sections through a synaptic bouton (b) synapsing (arrowhead) with a dendritic spine (s). Scale bar, 0.5 μm. (*B*) 3D reconstruction of the bouton and spine shown in *A* made from serial images. (*C*) Relationship between PSD area and synaptic contact zone area for excitatory synapses ($n = 34$) in L2/3 of spared cortex. Line represents the fit from the generalized linear model: PSD area = 0.009 + 0.53 (contact zone area); explained deviance 89%, $^{***}P < 0.001$ for all synapses.

We found that contact zones at putative synapses between L2/3 pyramidal neurons were 60% larger in spared cortex (215 [145–476] voxels, $n = 44$) than in control cortex (134 [94–203] voxels, $n = 40$; $P < 0.001$, *t*-test; Fig. 3*B*, Supplementary Fig. S6*A*,*B*; Supplementary Results). The distribution of contact zone size was tilted toward larger values in spared cortex ($P = 0.006$, Kolmogorov–Smirnov test; Fig. 4*B*). Furthermore, the mean contact zone size per connection was 137% larger in spared cortex (337 ± 57 voxels, $n = 12$) than in control cortex (142 ± 19 voxels, $n = 13$; $P = 0.003$, *t*-test). Similar results were found when our analyses were repeated with the maximum contact area in a single optical slice rather than the volume of the contact zone (Supplementary Fig. S6*C*,*D*). Contact zone size in spared cortex increased with the duration of whisker deprivation (Supplementary Fig. S5*C*). The dendritic location of the putative synapse did not affect the contact zone size (Supplementary Fig. S7). Taken together, these data suggested that there was a progressive increase in contact zone size at putative synapses forming strengthened connections in spared cortex. Furthermore, this finding could not be attributed to just a subset of those contacts becoming much bigger (Supplementary Fig. S8).

EM studies show that the sizes of many synaptic structures are correlated, for example, the volume of the postsynaptic spine with the area of the postsynaptic density, although variability is greater at bigger synapses (Harris and Stevens 1989; Schikorski and Stevens 1999). In our fluorescence images, we found that the size of the contact zone expanded linearly with increases in the volume of the varicosity (Fig. 3*C*; slope, 313 voxels μm^{-3}, $P < 0.001$; Supplementary Results). This relationship was not affected by deprivation status ($P = 0.16$). The relationship between dendritic spine volume and contact zone size was also linear although the slope was greater for spines in spared cortex than for spines in control cortex (control slope 140 voxels μm^{-3}, $P < 0.001$; spared slope 265 voxels μm^{-3}, $P = 0.002$; Supplementary Results; Fig. 3*D*). We checked that this result was robust by repeating the analysis after removing the 4 largest spines from the data set and found that the slopes were similar to those obtained for the full data set and remained statistically significant (Supplementary Results). We found a linear relationship between varicosity and spine volume (Supplementary Fig. S9, $P < 0.001$, explained deviance 55%), as reported for other central synapses (Schikorski and Stevens 1999). The spine–varicosity relationship was not modified by deprivation status (Supplementary Fig. S9, $P = 0.60$). Taken together, our findings suggest that the enlargement of varicosities and spines was coordinated across each strengthened putative synapse to expand the contact zone (Lisman and Harris 1993).

Contact Zone Size Scales with Synapse Size

We explored how contact between an axon and a spine is related to the size of synapses by performing serial section EM through a volume of 227 μm^3 of L2/3 in spared barrel cortex. The area of all contacts ($n = 92$) was measured in 3D (Materials and Methods). Synapses were present at 34 contacts. All contact zones showed a synapse if the contact area was >0.13 μm^2, which was the area of the biggest nonsynaptic contact (Supplementary Results). Only 2 synaptic contacts had contact zones < 0.13 μm^2. Hence, the vast majority (32 of 34, 94%) of synaptic contacts were larger than the biggest nonsynaptic contact.

At synapses, the contact zone between a presynaptic varicosity and a postsynaptic dendrite is much larger than the region of the synapse where neurotransmission occurs, that is, the presynaptic active zone and PSD. Therefore, we further analyzed our EM measurements of synapses and investigated the relationship between the size of the contact zone and the size of the PSD (Fig. 4*A*,*B*; Supplementary Results). We found a strong linear relationship between the area of the contact zone and the area of the PSD for both simple (disc-like) and complex (e.g. perforated) PSDs (slope, $\beta_1 = 0.53 \pm 0.04$, $P < 0.001$, explained deviance 89%, $n = 34$ synapses, generalized linear model, Materials and Methods; Fig. 4*C*). This indicates that contact zone size was tightly related to PSD size at presumed excitatory synapses. We concluded that the size of the contact zone between a presynaptic varicosity and a postsynaptic dendrite can be used as an index of synapse size.

Altered Presynaptic and Postsynaptic Functions Strengthen Synaptic Transmission in Spared Cortex

We next explored whether the expansion of the contact zone is linked to experience-dependent changes in synaptic function at strengthened connections. We have reported previously that the number of putative synapses per connection does not alter in spared cortex (Cheetham et al. 2007). Hence, synaptic strengthening could result from enhanced presynaptic release and/or increased postsynaptic response size. Presynaptic function was probed by studying failures of neurotransmission, which occur when none of the synapses forming a connection release neurotransmitter. We found that the probability of failure at excitatory connections between pairs of L2/3 pyramidal neurons was significantly lower in spared cortex (0.00 [0.00–0.08], $n = 10$; Materials and Methods) than that in control cortex (0.34 [0.06–0.59], $n = 13$; $P = 0.020$, Mann–Whitney rank sum test; Fig. 5*A*,*B*). Furthermore, the coefficient of variation of EPSP responses was significantly lower for connections in spared cortex

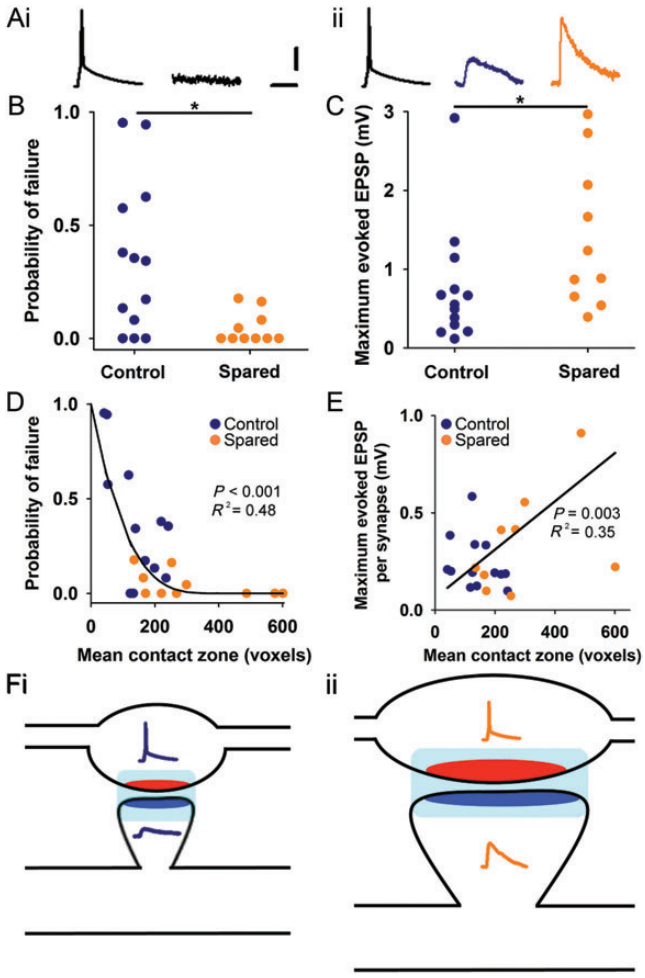

Figure 5. Excitatory connections in spared cortex are stronger and more reliable. (*A*) Example recordings of: (i) presynaptic action potential and postsynaptic failure; (ii) presynaptic action potential and maximum evoked uEPSPs in control (blue) and spared (orange) cortex (single traces). Scale bars: 40 mV, 0.5 mV; 10 ms. (*B*) Scatterplot of probability of failure. $^*P = 0.020$, Mann–Whitney test. (*C*) Scatterplot of maximum evoked uEPSP amplitude. $^*P = 0.032$, *t*-test. (*D*) Relationship between mean contact zone size and probability of failure. Curve represents the power fit to data, $y = (1–0.0017x)^{3.65}$. (*E*) Relationship between mean contact zone size and maximum evoked uEPSP amplitude per synapse. Line represents linear regression fit to all data points; Maximum evoked uEPSP amplitude = 0.0629 + 0.0012(mean contact zone size). $n = 13$ control and 10 spared connections. (*F*) Schematic showing that naïve synapses (i; active zone, red; postsynaptic density, blue; contact zone, cyan) become functionally stronger and structurally larger in spared cortex (ii).

(0.36 [0.25–0.59], $n = 10$) than that in control cortex (0.65 [0.32–1.40], $n = 13$; $P = 0.028$, Mann–Whitney rank sum test). Hence, our data suggest that putative synapses with larger contact zones at strengthened local excitatory connections in L2/3 of spared cortex have a higher probability of release, resulting in more reliable neurotransmission.

To investigate the postsynaptic response size, we measured the maximum response evoked by a connection, which occurs when all of the synapses forming the connection release neurotransmitter. We first validated this method for connections between pairs of L2/3 pyramidal neurons. We raised the extracellular calcium concentration from 2 to 5 mM to increase the presynaptic release probability and measured the effect on synaptic transmission and the maximum evoked uEPSP amplitude. This increase in extracellular calcium concentration resulted in a decrease in the probability of failure for the first uEPSP in the stimulus train (2 mM, 0.31 ± 0.08; 5 mM, 0.06 ± 0.04; $P = 0.010$, paired *t*-test, $n = 5$ connections), indicating that baseline presynaptic release probability had increased. However, the maximum evoked uEPSP amplitude recorded sequentially in 2 and 5 mM extracellular calcium did not change (2 mM, 0.45 ± 0.05 mV; 5 mM, 0.45 ± 0.03 mV; $P = 0.92$, paired *t*-test, $n = 5$ connections). We concluded that the maximum evoked uEPSP amplitude is not significantly affected by changes in release probability at local excitatory connections in L2/3 and, therefore, provides a good measure of the postsynaptic response when all synapses forming the connection release neurotransmitter.

We then tested the effect of altered sensory experience on the maximum evoked uEPSP amplitude. The maximum evoked uEPSP amplitude was significantly larger for connections in spared cortex (1.06 [0.65–2.07] mV, $n = 10$) than that in control cortex (0.55 [0.27–0.84] mV, $n = 13$; $P = 0.032$, *t*-test; Fig. 5*C*). These findings indicate that postsynaptic responses are larger in spared cortex, as would be predicted for synapses formed on larger dendritic spines (Fifková and Van Harreveld 1977; Matsuzaki et al. 2004; Park et al. 2004).

Structure–Function Relationship at Neocortical Synapses

Our data indicate that behavioral experience resulted in both functional strengthening and expansion of contact zones at putative synapses between L2/3 pyramidal neurons in spared cortex. Therefore, we next explored the relationship between contact zone size and function at these putative synapses. We modeled each putative synapse forming a connection as a theoretical, "average" synapse, whose properties were the mean of all the synapses forming the same connection, equivalent to a simple binomial model in quantal analysis. This model eliminates any variability between synapses comprising a connection. We related presynaptic structure and function by deriving a relationship (Materials and Methods) between the mean contact zone size and the probability of failure at a connection:

$$\text{Probability of failure} = (1 - k(\text{mean contact zone size}))^n$$

where n is the anatomically determined number of putative synapses forming the connection and k is a constant. The derived equation gave a good fit to all data points (Fig. 5*D*, $P < 0.001$, $R^2 = 0.48$), suggesting that contact zone size and probability of release co-vary in the mature cortex.

To investigate the postsynaptic structure–function relationship, we first estimated the EPSP amplitude evoked by an average synapse by dividing the maximum evoked EPSP amplitude by the number of putative synapses comprising the connection. The mean postsynaptic response evoked by an average synapse was linearly related to mean contact zone size in the pooled data (Fig. 5*E*; $P = 0.003$, $R^2 = 0.35$, linear regression). This finding indicates that contact zone size and postsynaptic response amplitude co-vary in the mature cortex.

Discussion

We investigated how the structure of synaptic contacts is modified when the synaptic connections between neurons undergo experience-dependent strengthening. Our findings show that the varicosities, spines, and the interposed contact zones forming strengthened excitatory cortical connections

are larger following weeks of altered sensory experience in vivo (Fig. 5*F*). Importantly, the differences in function of strengthened synapses paralleled the structural modifications. Hence, synapse structure contains information on differences in synaptic function induced by behavioral experience. The greater reliability of strengthened connections that we report is consistent with the increased probability of neurotransmitter release from presynaptic terminals and the increased maximum evoked uEPSP amplitude per connection indicates that the postsynaptic response to neurotransmitter release is enhanced. Pansynaptic enlargement, therefore, provides a mechanism by which increases in both presynaptic and postsynaptic strength can be stably maintained in the mature cortex.

The larger size of synaptic contacts that we report could be due to the enlargement of existing synaptic contacts or the growth of new, larger synapses. We have shown previously that the number of dendritic spines on L2/3 pyramidal neurons in spared cortex is not affected by sensory experience (Cheetham et al. 2007). This suggests that growth of new, larger synapses would be offset by loss of smaller, weaker synapses to keep spine number constant. L2/3 pyramidal neurons in the mature cortex undergo a low level of synapse turnover (Holtmaat et al. 2005; De Paola et al. 2006), which is increased by altering sensory experience (Holtmaat and Svoboda 2009) and may contribute to memory formation (Cheetham et al. 2008; Hofer et al. 2009; Xu et al. 2009; Yang et al. 2009). Typically, new synapses are formed by thin spines with small heads (Knott et al. 2006). Hence, our data, which show generalized spine expansion, indicate that experience-dependent growth of new synapses should at least parallel the enlargement of existing synapses. However, our data cannot distinguish the relative contributions of the enlargement of existing synapses and the growth of new synapses. This will require technological advances to permit longitudinal super-resolution imaging deep in the living brain (Berning et al. 2012).

Role of Presynaptic Structure in Synaptic Strengthening

The hypothesis that mature presynaptic terminals remodel during synaptic strengthening (Hebb 1949) has received surprisingly little attention. Strengthening of presynaptic function may be a feature of late LTP in the hippocampus (Bayazitov et al. 2007). However, EM studies have found little evidence for the enlargement of axonal boutons within 1 day of LTP induction (Fifková and Van Harreveld 1977; Chang and Greenough 1984). Our data demonstrate that the expansion of presynaptic terminals is an integral part of the structural plasticity that accompanies experience-dependent synaptic strengthening in vivo. Furthermore, the remodeling of synaptic boutons in the mature cortex occurred over days to weeks, mirroring the strengthening of local excitatory connections in spared cortex (Cheetham et al. 2007). Hence, the discrepancy between our findings and those following hippocampal LTP may be attributable to the kinetics of structural remodeling in mature cortex and/or a requirement for repeated or prolonged periods of altered input before remodeling of axonal boutons becomes evident.

How are structure and function linked at presynaptic terminals? The probability of release at central synapses is widely thought to be directly related to the number of synaptic vesicles that are docked at the presynaptic active zone (Dobrunz and Stevens 1997; Schikorski and Stevens 2001), which is, in turn, strongly correlated with the area of the active zone and with bouton volume (Pierce and Lewin 1994; Harris and Sultan 1995; Schikorski and Stevens 1997; Murthy et al. 2001). In spared cortex, we found that varicosity volumes were larger, the coefficient of variation of postsynaptic responses was lower, and the probability of failure of neurotransmission had decreased. Hence, our structural and functional findings are consistent and indicate that the probability of release had increased at excitatory synapses between L2/3 pyramidal neurons in spared cortex.

Role of Postsynaptic Structure in Synaptic Strengthening

Many previous studies of synaptic structural plasticity have focused on remodeling of postsynaptic dendritic spines. Early EM studies showed mixed effects of LTP on spine size (Fifková and Van Harreveld 1977; Chang and Greenough 1984; Sorra and Harris 1998; Yuste and Bonhoeffer 2001), possibly due to the difficulty of identifying potentiated synapses (Harris et al. 2003). More recently, live imaging studies of cultured hippocampal neurons have shown rapid, input-specific spine enlargement induced by LTP (Lang et al. 2004; Matsuzaki et al. 2004; Park et al. 2004; Kopec et al. 2006). Some studies found that spine enlargement lasts for >1 h at small spines, but is lost within tens of minutes at larger spines (Matsuzaki et al. 2004; Tanaka et al. 2008). This led to the proposal that small spines act as "learning spines" and larger spines are "memory spines" (Kasai et al. 2003; Matsuzaki et al. 2004). However, other studies have reported sustained (>1 h) expansion of spines of all sizes using a range of LTP-induction protocols (Kopec et al. 2006; Steiner et al. 2008; Yang et al. 2008; Bozdagi et al. 2010).

The maturity of the tissue may also affect structural remodeling of spines. Persistent LTP-induced spine enlargement has been difficult to elicit in mature hippocampus in vitro (Sorra and Harris 1998; Lang et al. 2004), although it has been reported more recently (Bozdagi et al. 2010). Dendritic spine enlargement in vivo has been described on pyramidal neuron apical tufts in layer 1 of the neocortex after motor training (Harms et al. 2008) or repeated episodes of monocular deprivation (Hofer et al. 2009). However, when motor training lasted only a few days, spine expansion was not maintained, suggesting that it can be transient (Harms et al. 2008). We found that dendritic spines at putative synapses forming strengthened connections in the mature neocortex were larger following weeks of altered in vivo sensory experience. Furthermore, our results indicate that all spine types are modified by prolonged periods of altered sensory experience in vivo. Taken together, our findings support the view that all spine types are capable of persistent enlargement in the mature brain.

EM reconstructions show that spine volume, PSD area, and AMPA receptor number are all highly correlated at central synapses (Harris and Stevens 1989; Kharazia and Weinberg 1999; Schikorski and Stevens 1999; Knott et al. 2006; Arellano et al. 2007). The enhanced postsynaptic response and enlarged dendritic spines that we found both suggest that there is a persistent increase in AMPA receptor number at local excitatory synapses onto L2/3 pyramidal neurons after prolonged behavioral experience in mature animals.

Expansion of Contact Zones at Strengthened Synapses

We found that contact zones between pyramidal neurons were larger at strengthened connections in spared cortex. However, our EM data indicate that neurons also form nonsynaptic contacts, which are usually smaller than synapses (Supplementary Results). These nonsynaptic contacts would appear as overlaps in our fluorescence images and could confound interpretation of our results. We addressed this issue by combining high-resolution imaging, image deconvolution, and stringent criteria for identifying putative synapses. We have previously validated our methods by analyzing fluorescence overlaps between pairs of L2/3 pyramidal neurons that were not connected electrophysiologically and found a false-positive rate of only 5% (Cheetham et al. 2007). Hence, the vast majority of contact zones that we report are the sites of synapses.

Our EM data showed a strong linear relationship between contact zone size and PSD area, indicating that they are tightly coupled. Hence, the enlargement of the contact zone that we found in our fluorescence images suggests that PSDs are also expanded at strengthened connections.

Coordinated Presynaptic and Postsynaptic Enlargement

Studying either presynaptic or postsynaptic structures in isolation provides an incomplete picture of structural synaptic remodeling. We imaged both the presynaptic and postsynaptic structures forming individual putative synapses and their interposed contact zones. Contact zone size was linearly related to both varicosity and spine volumes at individual putative synapses in the adult cortex. Our data suggest that presynaptic and postsynaptic structural remodeling is coordinated to expand the contact zone and PSD at individual synapses (Lisman and Harris 1993). The coordinated enlargement of apposed presynaptic and postsynaptic terminals could be implemented in many ways, for example, by transsynaptic signaling via synaptic cell adhesion molecules, such as neurexin–neuroligin (Choi et al. 2011), N-cadherin (Bozdagi et al. 2010; Mendez et al. 2010), integrins (Chavis and Westbrook 2001), neural cell adhesion molecules (Dalva et al. 2007), or via retrograde messengers (Regehr et al. 2009). However, the enlargement of presynaptic and postsynaptic terminals in the mature cortex need not be precisely temporally matched, nor employ the same mechanisms. Determination of the precise timing of the enlargement of varicosities and their apposed spines at synaptic contacts will require longitudinal super-resolution imaging deep in the living brain (Berning et al. 2012). Unraveling how structure and function are coordinated across the entire synapse in the adult brain will provide insights into how synapse structure supports synaptic computation.

Supplementary Material

Supplementary material can be found at: http://www.cercor.oxfordjournals.org/

Funding

This work was supported by the King's Medical Research Trust (C.E.J.C.), Medical Research Council PhD studentships (S.J.B. and G.A.), and a Wellcome Trust Senior Clinical Fellowship (G.T.F.). Funding to pay the Open Access publication charges for this article was provided by the Wellcome Trust.

Notes

We thank Martin Hammond for preliminary data, and Peter Giese, Frank Hirth, and Gerry Hammond for comments. *Conflict of Interest*: None declared.

References

Arellano JI, Benavides-Piccione R, DeFelipe J, Yuste R. 2007. Ultrastructure of dendritic spines: correlation between synaptic and spine morphologies. Front Neurosci. 1:131–143.

Barnes SJ, Finnerty GT. 2010. Sensory experience and cortical rewiring. Neuroscientist. 16:186–198.

Bayazitov IT, Richardson RJ, Fricke RG, Zakharenko SS. 2007. Slow presynaptic and fast postsynaptic components of compound long-term potentiation. J Neurosci. 27:11510–11521.

Becker N, Wierenga CJ, Fonseca R, Bonhoeffer T, Nagerl UV. 2008. LTD induction causes morphological changes of presynaptic boutons and reduces their contacts with spines. Neuron. 60:590–597.

Berning S, Willig KI, Steffens H, Dibaj P, Hell SW. 2012. Nanoscopy in a living mouse brain. Science. 335:551.

Bozdagi O, Wang XB, Nikitczuk JS, Anderson TR, Bloss EB, Radice GL, Zhou Q, Benson DL, Huntley GW. 2010. Persistence of coordinated long-term potentiation and dendritic spine enlargement at mature hippocampal CA1 synapses requires N-cadherin. J Neurosci. 30:9984–9989.

Chang FL, Greenough WT. 1984. Transient and enduring morphological correlates of synaptic activity and efficacy change in the rat hippocampal slice. Brain Res. 309:35–46.

Chavis P, Westbrook G. 2001. Integrins mediate functional pre- and postsynaptic maturation at a hippocampal synapse. Nature. 411:317–321.

Cheetham CE, Hammond MS, Edwards CE, Finnerty GT. 2007. Sensory experience alters cortical connectivity and synaptic function site specifically. J Neurosci. 27:3456–3465.

Cheetham CE, Hammond MS, McFarlane R, Finnerty GT. 2008. Altered sensory experience induces targeted rewiring of local excitatory connections in mature neocortex. J Neurosci. 28:9249–9260.

Choi YB, Li HL, Kassabov SR, Jin I, Puthanveettil SV, Karl KA, Lu Y, Kim JH, Bailey CH, Kandel ER. 2011. Neurexin-neuroligin transsynaptic interaction mediates learning-related synaptic remodeling and long-term facilitation in aplysia. Neuron. 70:468–481.

Dalva MB, McClelland AC, Kayser MS. 2007. Cell adhesion molecules: signalling functions at the synapse. Nat Rev Neurosci. 8:206–220.

De Paola V, Holtmaat A, Knott G, Song S, Wilbrecht L, Caroni P, Svoboda K. 2006. Cell type-specific structural plasticity of axonal branches and boutons in the adult neocortex. Neuron. 49:861–875.

Dobrunz LE, Stevens CF. 1997. Heterogeneity of release probability, facilitation, and depletion at central synapses. Neuron. 18:995–1008.

Dyson SE, Jones DG. 1980. Quantitation of terminal parameters and their inter-relationships in maturing central synapses: a perspective for experimental studies. Brain Res. 183:43–59.

Elhanany E, White EL. 1990. Intrinsic circuitry: synapses involving the local axon collaterals of corticocortical projection neurons in the mouse primary somatosensory cortex. J Comp Neurol. 291:43–54.

Fifková E, Van Harreveld A. 1977. Long-lasting morphological changes in dendritic spines of dentate granular cells following stimulation of the entorhinal area. J Neurocytol. 6:211–230.

Fox K, Wong RO. 2005. A comparison of experience-dependent plasticity in the visual and somatosensory systems. Neuron. 48:465–477.

Geinisman Y. 2000. Structural synaptic modifications associated with hippocampal LTP and behavioral learning. Cereb Cortex. 10:952–962.

Greenough WT, Bailey CH. 1988. The anatomy of a memory: convergence of results across a diversity of tests. Trends Neurosci. 11:142–147.

Guic-Robles E, Valdivieso C, Guajardo G. 1989. Rats can learn a roughness discrimination using only their vibrissal system. Behav Brain Res. 31:285–289.
Harms KJ, Rioult-Pedotti MS, Carter DR, Dunaevsky A. 2008. Transient spine expansion and learning-induced plasticity in layer 1 primary motor cortex. J Neurosci. 28:5686–5690.
Harris JA, Petersen RS, Diamond ME. 1999. Distribution of tactile learning and its neural basis. Proc Natl Acad Sci USA. 96:7587–7591.
Harris KM, Fiala JC, Ostroff L. 2003. Structural changes at dendritic spine synapses during long-term potentiation. Philos Trans R Soc Lond B Biol Sci. 358:745–748.
Harris KM, Jensen FE, Tsao B. 1992. Three-dimensional structure of dendritic spines and synapses in rat hippocampus (CA1) at postnatal day 15 and adult ages: implications for the maturation of synaptic physiology and long-term potentiation. J Neurosci. 12:2685–2705.
Harris KM, Stevens JK. 1989. Dendritic spines of CA 1 pyramidal cells in the rat hippocampus: serial electron microscopy with reference to their biophysical characteristics. J Neurosci. 9:2982–2997.
Harris KM, Sultan P. 1995. Variation in the number, location and size of synaptic vesicles provides an anatomical basis for the nonuniform probability of release at hippocampal CA1 synapses. Neuropharmacology. 34:1387–1395.
Hebb DO. 1949. Organization of behavior: a neuropsychological theory. New York (NY): John Wiley & Sons.
Hofer SB, Mrsic-Flogel TD, Bonhoeffer T, Hubener M. 2009. Experience leaves a lasting structural trace in cortical circuits. Nature. 457:313–317.
Holtmaat A, Svoboda K. 2009. Experience-dependent structural synaptic plasticity in the mammalian brain. Nat Rev Neurosci. 10:647–658.
Holtmaat AJGD, Trachtenberg JT, Wilbrecht L, Shepherd GM, Zhang XQ, Knott GW, Svoboda K. 2005. Transient and persistent dendritic spines in the neocortex in vivo. Neuron. 45:279–291.
Jones DG, Calverley RK. 1991. Perforated and non-perforated synapses in rat neocortex: three-dimensional reconstructions. Brain Res. 556:247–258.
Kasai H, Matsuzaki M, Noguchi J, Yasumatsu N, Nakahara H. 2003. Structure-stability-function relationships of dendritic spines. Trends Neurosci. 26:360–368.
Kharazia VN, Weinberg RJ. 1999. Immunogold localization of AMPA and NMDA receptors in somatic sensory cortex of albino rat. J Comp Neurol. 412:292–302.
Kirov SA, Sorra KE, Harris KM. 1999. Slices have more synapses than perfusion-fixed hippocampus from both young and mature rats. J Neurosci. 19:2876–2886.
Knott GW, Holtmaat A, Wilbrecht L, Welker E, Svoboda K. 2006. Spine growth precedes synapse formation in the adult neocortex in vivo. Nat Neurosci. 9:1117–1124.
Kopec CD, Li B, Wei W, Boehm J, Malinow R. 2006. Glutamate receptor exocytosis and spine enlargement during chemically induced long-term potentiation. J Neurosci. 26:2000–2009.
Kopec CD, Real E, Kessels HW, Malinow R. 2007. GluR1 links structural and functional plasticity at excitatory synapses. J Neurosci. 27:13706–13718.
Landmann L, Marbet P. 2004. Colocalization analysis yields superior results after image restoration. Microsc Res Tech. 64:103–112.
Lang C, Barco A, Zablow L, Kandel ER, Siegelbaum SA, Zakharenko SS. 2004. Transient expansion of synaptically connected dendritic spines upon induction of hippocampal long-term potentiation. Proc Natl Acad Sci USA. 101:16665–16670.
Larkman AU. 1991. Dendritic morphology of pyramidal neurones of the visual cortex of the rat: III. Spine distributions. J Comp Neurol. 306:332–343.
Lisman JE, Harris KM. 1993. Quantal analysis and synaptic anatomy–integrating two views of hippocampal plasticity. Trends Neurosci. 16:141–147.
Markram H, Lubke J, Frotscher M, Roth A, Sakmann B. 1997. Physiology and anatomy of synaptic connections between thick tufted pyramidal neurones in the developing rat neocortex. J Physiol (Lond). 500:409–440.
Martin SJ, Grimwood PD, Morris RG. 2000. Synaptic plasticity and memory: an evaluation of the hypothesis. Annu Rev Neurosci. 23:649–711.
Matsuzaki M, Honkura N, Ellis-Davies GCR, Kasai H. 2004. Structural basis of long-term potentiation in single dendritic spines. Nature. 429:761–766.
Mendez P, De RM, Poglia L, Klauser P, Muller D. 2010. N-cadherin mediates plasticity-induced long-term spine stabilization. J Cell Biol. 189:589–600.
Murthy VN, Schikorski T, Stevens CF, Zhu Y. 2001. Inactivity produces increases in neurotransmitter release and synapse size. Neuron. 32:673–682.
Pan W. 2001. Akaike's information criterion in generalized estimating equations. Biometrics. 57:120–125.
Park M, Penick EC, Edwards JG, Kauer JA, Ehlers MD. 2004. Recycling endosomes supply AMPA receptors for LTP. Science. 305:1972–1975.
Peters A, Kaiserman-Abramof IR. 1970. The small pyramidal neuron of the rat cerebral cortex. The perikaryon, dendrites and spines. Am J Anat. 127:321–355.
Peters A, Kaiserman-Abramof IR. 1969. The small pyramidal neuron of the rat cerebral cortex. The synapses upon dendritic spines. Z Zellforsch Mikrosk Anat. 100:487–506.
Pierce JP, Lewin GR. 1994. An ultrastructural size principle. Neuroscience. 58:441–446.
Ramón y Cajal S. 1894. The Croonian lecture: La fine structure des centres nerveux. Proc R Soc Lond. 55:444–468.
Regehr WG, Carey MR, Best AR. 2009. Activity-dependent regulation of synapses by retrograde messengers. Neuron. 63:154–170.
Schikorski T, Stevens CF. 2001. Morphological correlates of functionally defined synaptic vesicle populations. Nat Neurosci. 4:391–395.
Schikorski T, Stevens CF. 1999. Quantitative fine-structural analysis of olfactory cortical synapses. Proc Natl Acad Sci USA. 96:4107–4112.
Schikorski T, Stevens CF. 1997. Quantitative ultrastructural analysis of hippocampal excitatory synapses. J Neurosci. 17:5858–5867.
Silver RA, Lübke J, Sakmann B, Feldmeyer D. 2003. High-probability uniquantal transmission at excitatory synapses in barrel cortex. Science. 302:1981–1984.
Sorra KE, Harris KM. 1998. Stability in synapse number and size at 2 hr after long-term potentiation in hippocampal area CA1. J Neurosci. 18:658–671.
Steiner P, Higley MJ, Xu W, Czervionke BL, Malenka RC, Sabatini BL. 2008. Destabilization of the postsynaptic density by PSD-95 serine 73 phosphorylation inhibits spine growth and synaptic plasticity. Neuron. 60:788–802.
Tanaka J, Horiike Y, Matsuzaki M, Miyazaki T, Ellis-Davies GC, Kasai H. 2008. Protein synthesis and neurotrophin-dependent structural plasticity of single dendritic spines. Science. 319:1683–1687.
Tanzi E. 1893. I fatti e le induzioni dell'odierna istologia del sistema nervoso. Riv Sper Fren Med Leg. 19:419–472.
Wallace W, Bear MF. 2004. A morphological correlate of synaptic scaling in visual cortex. J Neurosci. 24:6928–6938.
Wise SP, Fleshman JW Jr, Jones EG. 1979. Maturation of pyramidal cell form in relation to developing afferent and efferent connections of rat somatic sensory cortex. Neuroscience. 4:1275–1297.
Woolsey TA, Van der Loos H. 1970. The structural organisation of layer IV in the somatosensory region of mouse cerebral cortex. The description of a cortical field composed of discrete cytoarchitectonic units. Brain Res. 17:205–242.
Xu T, Yu X, Perlik AJ, Tobin WF, Zweig JA, Tennant K, Jones T, Zuo Y. 2009. Rapid formation and selective stabilization of synapses for enduring motor memories. Nature. 462:915–919.
Yang G, Pan F, Gan WB. 2009. Stably maintained dendritic spines are associated with lifelong memories. Nature. 462:920–924.
Yang Y, Wang XB, Frerking M, Zhou Q. 2008. Spine expansion and stabilization associated with long-term potentiation. J Neurosci. 28:5740–5751.
Yuste R, Bonhoeffer T. 2001. Morphological changes in dendritic spines associated with long-term synaptic plasticity. Annu Rev Neurosci. 24:1071–1089.
Zucker RS, Regehr WG. 2002. Short-term synaptic plasticity. Annu Rev Physiol. 64:355–405.